The cell lysates were incubated sequentially with preimmune sera, polyclonal rabbit antibodies to human IL-1β, or anti-p20 ICE and protein A–agarose. After extensive washes, the adsorbed proteins were eluted by boiling the beads in SDS-PAGE sample buffer and analyzed by SDS-PAGE and autoradiography.

13. The ICE homologs and p35 were expressed in *E. coli* under the control of the λ pL promoter. ICH-1 (*7*) and CPP32α (*8*) contained a polyhistidine linker and were purified by IMAC as described for ICH-2; p35 was purified by chromatography on Q-Sepharose, Mono-Q, and Superdex-75.
14. Colorimetric assays were performed in 96-well plates by incubating enzyme in assay buffer [100 mM Hepes (pH 7.5), 0.5 mM EDTA, 20% glycerol, and 5 mM dithiothreitol] with *N*-acetyl-Tyr-Val-Ala-Asp-*p*-nitroanilide (AcYVAD-pNA) as substrate for ICE and ICH-2 or with *N*-acetyl-Asp-Glu-Val-Asp-*p*-nitroanilide (AcDEVD-pNA) (Quality Controlled Biochemicals, Hopkinton, MA) as substrate for ICH-1 and CPP32. Absorbance at 405 nm was monitored at 37°C for 30 min.
15. L. Shi, C. M. Kam, J. C. Powers, R. Aebersold, A. H. Greenberg, *J. Exp. Med.* **176**, 1521 (1992).
16. Proteins were separated on gels containing a 10 to 20% gradient of acrylamide (Integrated Separations Science, Natick, MA) in tris-tricine buffer under reducing conditions. For immunoblot analysis, the proteins were electrophoretically transferred onto nitrocellulose and the membranes were blocked, washed, and incubated in purified rabbit immunoglobulin G (IgG) followed by donkey antibodies to horseradish peroxidase–conjugated rabbit IgG (Amersham). Immunoblots were developed by enhanced chemiluminescence (Amersham). Rabbit antisera to p35 were produced against residues 75 to 299 fused to trpE of *E. coli*. ICE has a k_{cat} value of 0.5 mol aminomethylcoumarin (Amc) mol^{-1} s^{-1} compared to 1 mol Amc mol^{-1} s^{-1} reported previously (*27*). When approximately equal amounts of ICE and p35 protein were used, only about half of the p35 was cleaved (Fig. 2B, lane 3), consistent with the presence of some inactive enzyme in the preparations used.
17. N. Bump, unpublished results.
18. N. P. C. Walker *et al.*, *Cell* **78**, 343 (1994); K. P. Wilson *et al.*, *Nature* **370**, 270 (1994).
19. DNAs encoding p35 or human proIL-1β were subcloned into pSVb. The TNT T7-coupled reticulocyte system (Promega) was used to generate proteins labeled with [^{35}S]methionine (15 mCi/ml, Amersham). Radiolabeled p35 was incubated with ICE at 30°C for 30 min, and the reactions were stopped by heating in SDS-PAGE sample buffer. For the reassociation experiments, the mixtures that contained ICE, AcYVK(biotin)D-CHO, and ^{35}S-labeled p35 or human proIL-1β were incubated with streptavidin-agarose. The beads were washed, adsorbed proteins were eluted by boiling in 1% SDS, and the labeled proteins were detected by autoradiography after SDS-PAGE.
20. Equimolar amounts of *N*-acetyl-Tyr-Val-Lys-Asp-aldehyde (Bachem Bioscience) and (biotinoyl-ε-aminocaproyl)-ε-aminocaproic acid *N*-hydroxysuccinimide ester (Molecular Probes) were combined in a 1:1 mixture of ethanol and 100 mM sodium borate (pH 8.5) for 80 min at room temperature. The biotinylated product was separated from the starting peptidyl aldehyde by reversed-phase high-performance liquid chromatography (HPLC). The biotinylated peptide aldehyde AcYVK(biotin)D-CHO inhibited ICE with a K_i of less than 1 nM.
21. N. Bump, unpublished results.
22. Complementary DNA fragments encoding either the p32 or p45 forms of human ICE were inserted into pVL1393 (Invitrogen). The transfer plasmid was cotransfected into SF-9 cells with linearized AcMNPV DNA by means of the BaculoGold system (Pharmingen). Recombinant virus expressing ICE (BV-ICE) was purified by several rounds of infection.
23. For production of ICE, SF-9 cells were infected at a multiplicity of infection of 2 to 5 with recombinant virus stock with a titer of 1×10^8 plaque-forming units per milliliter. The medium was harvested when cell viability was between 0 and 20% and concentrated on SP-Sepharose HP (Pharmacia). We added 10 mM dithiothreitol, 3 mM AcYVK(biotin)D-CHO, and streptavidin-agarose to the eluted protein. Affinity-purified enzyme was eluted by addition of 100 mM Hepes, 20% glycerol, 100 mM hydroxylamine, 10 mM oxidized glutathione (GSSG), and 0.5 mM EDTA (pH 7.5).
24. We introduced six histidine residues at the NH_2-terminus of p32 ICE with the use of a Lys-Ser-Gly-Ala-Asp-Asp-Asp-Asp-Asp-Lys linker and produced recombinant virus expressing this construct (N-His-ICE) as described (*22*). Culture medium from SF-9 cells infected with this virus was loaded onto HiTrap Chelating Sepharose (Pharmacia) charged with $NiCl_2$, and the N-His-ICE–p35 complex was eluted by addition of 150 mM imidazole.
25. Proteins were separated by SDS-PAGE on 14% acrylamide gels and transferred onto ProBlott (Applied Biosystems). After detection by Ponceau-S staining, the bands of interest were excised and NH_2-terminal sequencing was performed.
26. C. Ferenz, unpublished results. Proteins were transferred onto nitrocellulose membrane and digested with trypsin (Promega). The tryptic peptides were separated by reversed-phase HPLC and sequenced on an Applied Biosystems 477A pulse-liquid phase automated sequencer.
27. N. A. Thornberry *et al.*, *Nature* **356**, 768 (1992).
28. Complementary DNA encoding the p32 form of ICE was subcloned into a pBluescript II KS$^+$ (Stratagene) derivative under the control of the bacteriophage λ pL promoter. We constructed a second plasmid with the p35 gene inserted upstream of the ICE gene, thus creating a bicistronic message for coexpression in *E. coli* mm294 cells. Cells were grown at 29°C to an optical density of 0.6 at 600 nm and were induced to synthesize recombinant proteins by raising the temperature to 40°C.
29. The plasmid pHSP35VI$^+$ contains p35 under the control of the *Drosophila Hsp70* promoter in a pBluescript-based (Stratagene) plasmid vector (*2*). This promoter is constitutively transcribed upon transfection in SF-21 cells and can be stimulated further by heat shock (*2, 32*). Plasmid pHSPICE32VI$^+$ is identical to pHSP35VI$^+$ except that it contains p32 ICE instead of p35. SF-21 cells or TN-368 cells (5×10^5 to 6×10^5 per 35-mm dish) were transfected with plasmid DNA with the use of Lipofectin (Bethesda Research Laboratories). At 20 hours posttransfection, cells were heat-shocked for 30 min at 42°C. The media were removed 10 to 12 hours after heat shock, the cells were resuspended in 500 μl of phosphate-buffered saline containing 0.04% trypan blue, and viable cells were counted with a hemocytometer. Transfections were repeated in triplicate and viable cells in four grids of the hemocytometer were counted for each replicate.
30. S. Seshagiri, unpublished results. SF-21 or TN-368 cells were transfected with pBluescript, pHSPICE32VI$^+$, and pHSP35VI$^+$ and total DNA was isolated, electrophoresed through an agarose gel, and visualized by ethidium bromide staining.
31. C. A. Ray *et al.*, *Cell* **69**, 597 (1992); L. T. Quan, A. Caputo, R. C. Bleackley, D. J. Pickup, G. S. Salvesen, *J. Biol. Chem.* **270**, 10377 (1995).
32. T. D. Morris and L. K. Miller, *J. Virol.* **66**, 7397 (1992).
33. We thank L. Perron for manuscript preparation and B. Seed of Harvard Medical School for the MNC(neo) vector. Supported in part by U.S. Public Health Service grant AI 38262 to L.K.M.

16 May 1995; accepted 4 August 1995

TECHNICAL COMMENTS

Honeybees and Magnetoreception

Chin-Yuan Hsu and Chia-Wei Li (*1*) propose that magnetite particles in the fat body of honeybees are part of a magnetic field sensory system used for navigation. They make the following statements that we think are in error or may have other interpretations.

1) Honeybees contain iron in "granules" only in the fat body. Iron granules have been described in honeybee midgut as well as the fat body (*2*). They are mineral concretions in vacuoles derived from the rough endoplasmic reticulum (RER) and form in response to iron in pollen in the diet.

2) Iron in honeybee fat body occurs in particles 7.5 nm in diameter. We have identified iron in holoferritin in the RER of many insects. Holoferritin has dense cores 7.5 nm in diameter (*3, 4*), the size of the particles mentioned by Hsu and Li. The dense masses in the iron granules look like hemosiderin degradation products of holoferritin described in other insects (*5*). Hsu and Li make no mention of ferritin or hemosiderin.

3) The fat body is innervated. Their scanning electron micrograph [figure 2B in (*1*)] illustrating innervation of a fat body shows a filamentous structure resembling a trachea. Hsu and Li do not mention the tracheae and tracheoles commonly observed on the surface of the fat body–oenocyte complex, or how they may be distinguished from nerves in scanning electron micrographs. Innervation of insect fat body has not been described. Should the honeybee fat body–oenocyte complex prove an exception, it may be related to the control of wax secretion rather than to magnetotaxis. The transmission electron micrograph of a nerve ending in a fat body [figure 2C in (*1*)] shows the synaptic vesicles appropriate for an excitatory nerve rather than the sensory nerve required for a magnetotactic organ.

4) Nerve endings in the fat body are stimulated through a transducer mechanism. We could find no structure corresponding to the proposed transducer complex needed to convert intracellular stress to extracellular nerve action potentials.

5) The granules are attached to cytoskeletal filaments that form the stress-activated part of the transducer complex. Honeybee vacuoles have no special attachment to cytoskeletal filaments (Fig. 1). Their bounding membranes resemble those of the rest of the RER. Preparations without osmication to preserve the cytoskeleton show filaments between mouse pancreas lamellate ER (*6*), but not around honeybee iron-containing vacuoles.

Iron concretions are abundant throughout honeybee fat body, as would be expect-

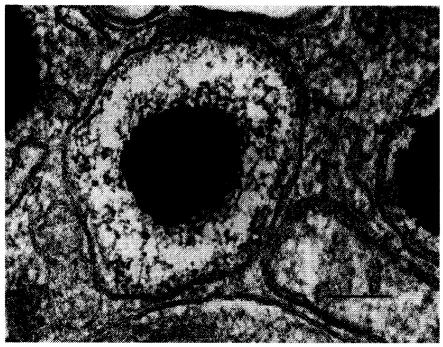

Fig. 1. Honeybee fat body. No special cytoskeletal filaments are observed connecting RER vacuoles containing iron concretions to hypothetical transducers for magnetotaxis. Bar, 0.1 μm.

ed for an insect subject to iron overload from the ingestion of iron-rich pollen, a major component of their diet. Bees on a pollen-poor diet lack fat body granules, but continue to contain some holoferritin (*2*). We found that the fat body of foraging honeybees contained vacuoles at all stages forming from the RER and the nuclear envelope, as would be expected if iron sequestration is a response to iron in the diet.

It appears to us that Hsu and Li may have misinterpreted their observations of honeybee fat body. In particular, they do not discuss the role of ferritin and the general function of insect fat body in iron metabolism (*4*). Holoferritin- and iron-containing granules are present in many insect tissues, especially when dietary iron is high or experimentally elevated. In honeybees the appearance of such granules is consistent with diet and involvement of the fat body with ferritin and its degradation products.

Helen Nichol
Michael Locke
Department of Zoology, University of Western Ontario, London, Ontario, Canada N6A 5B7
E-mail: mlocke@julian.uwo.ca

REFERENCES

1. C.-Y. Hsu and C.-W. Li, *Science* **265**, 95 (1994).
2. H. Raes, W. Bohyn, P. H. De Rycke, F. Jacobs, *Apidologie* **20**, 327 (1989).
3. M. Locke and H. Leung, *Tissue Cell* **16**, 739 (1984).
4. M. Locke and H. Nichol, *Annu. Rev. Entomol.* **37**, 195 (1992).
5. H. Nichol and M. Locke, *Tissue Cell* **22**, 767 (1990).
6. M. Locke, *J. Electron Microsc. Tech.* **29**, 1 (1994).

23 September 1994; accepted 9 May 1995

Studies of honeybee magnetoreception that provide anatomical and biophysical constraints on the insect receptor system contradict the conclusions of Hsu and Li in their report about iron granules in the abdominal trophocytes of honeybees (*1*). First, studies using ultrasensitive superconducting quantum-interference device magnetometers and transmission electron microscopy of extracts indicate that magnetite in honeybees is located primarily in the anterior, dorsal region of the abdomen, not in each abdominal segment as are the iron granules. This includes crystals of both single-domain (*2*) and superparamagnetic (*3*) size, as well as ordered sheets containing arrays of 15- to 20-nm superparamagnetic particles with electron diffraction patterns of magnetite (*4*).

Second, because large numbers of closely interacting superparamagnetic particles will display net magnetic behavior typical of larger grains (*5*), the magnetite particles postulated by Hsu and Li should have been detected by low-temperature magnetic warming experiments (*3*). The volume of superparamagnetic magnetite (4.4×10^{-15} ml) observed to be in each granule (*1*) should produce a moment of 1.1×10^{-15} Am^2 in these experiments. Because the total volume of the iron granules per bee is 2.5×10^{-5} ml (*6*) and each granule has a volume of 1.13×10^{-13} ml (*1*), each bee should have a total of about 2.2×10^{8} iron granules. This should have produced a moment of 2.3×10^{-7} Am^2, compared to the much lower measured value of 2×10^{-9} Am^2 (*3*). Hence, we doubt that the crystalline material identified by Hsu and Li (*1*) is magnetite.

Third, behavioral experiments with small magnetized wires glued at various locations on the surface of free-flying bees have explicitly tested the hypothesis that ferromagnetic magnetoreceptors are located in the anterior, dorsal region of the abdomen (*7*). Magnets positioned in this location impair the ability of the bees to respond to magnetic cues in discriminative choice experiments, whereas nonmagnetic control wires, or magnets positioned elsewhere (*7*), have no effect. Hence, we find no evidence to support the conclusion of Hsu and Li (*1*) that the ventral abdominal trophocytes could function as magnetoreceptors in honeybees.

Joseph L. Kirschvink
Division of Geological and Planetary Sciences, California Institute of Technology, Pasadena, CA 91125, USA
E-mail: krschvnk@caltech.edu
Michael M. Walker
School of Biological Sciences, University of Auckland, Private Bag, Auckland, New Zealand
E-mail: m.walker@auckland.ac.nz

REFERENCES

1. C.-Y. Hsu and C.-W. Li, *Science* **265**, 95 (1994).
2. J. L. Gould, J. L. Kirschvink, K. S. Deffeyes, *ibid.* **201**, 1026 (1978).
3. J. L. Kirschvink and J. L. Gould, *BioSystems* **13**, 181 (1981).
4. J. L. Kirschvink, J. Diaz-Ricci, M. H. Nesson, S. J. Kirschvink, *Magnetite-Based Magnetoreceptors: Ultrastructural, Behavioral, and Biophysical Studies* (Electric Power Research Institute, Palo Alto, CA, 1993).
5. V. V. Shcherbakova, *Earth Phys.* **14**, 308 (1978).
6. D. A. Kuterbach, B. Walcott, R. J. Reeder, R. B. Frankel, *Science* **218**, 695 (1982).
7. M. M. Walker and M. E. Bitterman, *J. Exp. Biol.* **141**, 447 (1989); *ibid.* **145**, 489 (1989).

28 December 1994; accepted 9 May 1995

Hsu and Li (*1*) conclude that some of the iron-containing granules present in the trophocytes of the honeybee abdomen contain superparamagnetic crystallites of magnetite. However, earlier studies by Kuterbach *et al.* (*2*) and by Hsu and Li (*3*) did not produce detectable electron diffraction patterns from these granules. Hsu and Li (*1*) do not present any electron diffraction pattern from the imaged crystallites. Their evidence for the presence of magnetite is based on Fourier transform optical analysis of the lattice fringes observed in their high-resolution transmission electron micrograph images [figure 1, B and C, in (*1*)]. Attempts to index the optical diffraction pattern from figure 1D in their report are necessarily crude; nevertheless, I have been unable to make the entire pattern consistent with a single crystal pattern from magnetite. Assuming that the electron microscope was accurately calibrated, relatively strong diffraction maxima with a spacing of 0.24 to 0.25 nm are evident. Although these maxima were indexed as 113,311, this single *d*-spacing is by itself insufficient to positively identify magnetite, much less distinguish between magnetite and either ferrihydrite, maghemite, or hematite.

That Hsu and Li did not obtain any electron diffraction pattern, despite the demonstration of lattice fringes, requires explanation. For a highly ordered crystal structure, the information in the sample that is converted into an image of the lattice fringes is the same as that which can be transformed into an electron diffraction pattern by an alternative arrangement of lens currents in the electron microscope. Hsu and Li estimate that the volume of "superparamagnetic magnetite" (that is, the crystalline domains) per granule is 4.4×10^{-15} cm^3, which is equivalent to a sphere more than 200 nm in diameter. Such a quantity of magnetite might be expected to provide ample material to produce a strong electron diffraction pattern. I readily obtained characteristic magnetite single crystal electron diffraction patterns from individual 40-nm magnetosomes in plastic-embedded sections of the magnetotactic bacterium *Magnetopirillum magnetotacticum* (unpublished results). The random arrangement of the individual crystallites within the honeybee iron granule should lead to the production of a typical powder pattern.

The formation of the honeybee iron granules by aggregation of 7.5-nm electron-

dense particles (*3*, *4*) suggests a potential explanation for the poor electron diffraction properties of the iron-containing material. The iron storage protein, ferritin, contains an electron-dense, 7.5-nm core composed of the poorly diffracting hydrous ferric oxide mineral, ferrihydrite (*5*). The formation of hemosiderin deposits in mammalian tissues (*6*) and the maturation of iron deposition granules in the dental epithelial tissues of Polyplacophoran molluscs (*7*) suggests that the protein shell of the ferritin molecule can be degraded to release the ferrihydrite cores. These finely divided cores may condense to yield iron-containing granules that resemble the structures described in honeybee trophocytes. The inherent small crystallite size will therefore necessarily produce a diffraction node "broadening" regardless of crystallinity. A clear diffraction pattern from an aggregation of ferrihydrite cores is not expected, although a crystallite size of 7.5 nm for the component particles is.

Michael H. Nesson
Department of Biochemistry and Biophysics, Oregon State University, Corvallis, OR 97331–7305, USA
E-mail: nessonm@bcc.orst.edu

REFERENCES

1. C.-Y. Hsu and C.-W. Li, *Science* **265**, 95 (1994).
2. D. A. Kuterbach, B. Walcott, R. J. Reeder, R. B. Frankel, *ibid.* **218**, 695 (1982).
3. C.-Y. Hsu and C.-W. Li, *J. Exp. Biol.* **180**, 1 (1993).
4. H. Raes, W. Bohyn, P. H. De Rycke, F. Jacobs, *Apidologie* **20**, 327 (1989).
5. K. M. Towe and W. F. Bradley, *J. Colloid Interface Sci.* **24**, 384 (1967); F. V. Chukhrov, B. B. Zvyagin, A. I. Gorshkov, L. P. Yermilova, V. V. Balashova, *Int. Geol. Rev.* **16**, 1131 (1973).
6. G. T. Matioli and R. F. Baker, *J. Ultrastr. Res.* **8**, 477 (1963); G. Hoy and A. Jacobs, *Br. J. Haematol.* **49**, 593 (1981); T. Iancu, *Mol. Aspects Med.* **6**, 1 (1982).
7. M. H. Nesson and H. A. Lowenstam, in *Magnetite Biomineralization and Magnetoreception in Organisms: A New Biomagnetism*, J. L. Kirschvink, D. S. Jones, B. J. MacFadden, Eds. (Plenum, New York, 1985), pp. 333–363.

12 January 1995; accepted 9 May 1995

Response: Nichol and Locke and Nesson suggest that the iron granules in the trophocytes of honeybees are derived from densely packed iron cores of degraded ferritin. Although our report (*1*) did not address the question of whether ferritin is directly involved in iron granule formation, this possibility has been explored (*2*). Calcium has been shown to be absent in ferritin and hemosiderin; however, x-ray microanalysis has indicated the presence of substantial amounts of calcium and phosphorus in iron granules (*2*). Furthermore, we did not detect any crystalline structures in newly deposited iron granules, and the superparamagnetic particles were observed only in matured iron granules (*1*). Our finding that the lattice fringes of the observed crystals often appear to extend the boundary of 7.5-nm electron-dense particles provides additional evidence that the superparamagnetic particles are probably not the ferritin iron cores (*1*). The use of immunoelectron microscopy at the early stage of iron granule formation should clarify this issue.

Nichol and Locke suggest that iron granules in the trophocytes of honeybees form in response to iron in the diet. However, although the rate of iron accumulation has been shown to be directly related to the amount of iron in the diet, the iron content of the fat body or of the whole bee reaches a maximum regardless of the amount of iron available for ingestion (*3*). Thus, the accumulation of iron appears to be physiologically regulated, not merely a response to high concentrations of iron in the diet. The observation that maximal iron accumulation occurred when honeybee workers begin foraging behavior (*3*, *4*) and that there is a distinct difference in the distribution of iron granules found among members of the hive (*4*) suggests that the iron granules may play a role in orientation.

Both the superconducting quantum-interference device analysis and the behavioral data on honeybees have shown that the magnetic detectors could be single domain magnetite or superparamagnetic particles; however, subsequent attempts to locate the detectors in situ and to characterize their cellular ultrastructure have been unsuccessful (*5*). The recent finding in iron granules of crystals of both single domain and superparamagnetic size, mentioned in the comment by Kirschvink and Walker, was also based on extracts of honeybees. Thus, the identification of superparamagnetic particles in situ is one of the major contributions of our report. The calculation by Kirschvink and Walker assumes that all of the iron granules have similar amounts of superparamagnetic particles, which is inconsistent with our observation. In our study (*1*), we identified superparamagnetic particles in only 4 out of 40 iron granules. Therefore, the extrapolation by Kirschvink and Walker to all particles is misleading. The high-resolution transmission electron microscopy (JEOL 400EX) gun that we used to examine the superparamagnetic particles is LaB_6. Because its diffraction probe is 2 to 3 μm in diameter (that is, much larger than the object under examination), a diffraction pattern is not expected. We are in the process of constructing a field emission gun with a much smaller probe, which we hope will generate a clear electron diffraction pattern.

We have observed cytoskeletons in close proximity to the iron deposition vesicle (IDV), with one end attached to an electron-dense rod on the IDV membrane in the worker bee (*1*, *3*). Both the cytoskeleton and attaching site are not abundant, hence they have to be examined carefully in ultrathin sections. The figure in the comment by Nichol and Locke does not disprove their existence.

In our report (*1*), the working hypothesis describing the mechanism whereby orienting iron granules generate signals that are relayed to the honeybee neural system is formulated on the basis of several fragmentary findings. Detailed analyses of the sensitivity of iron granules to Earth's magnetic field, the cytoskeletal system of the trophocyte, and the relation between the trophocyte and the neural system are necessary in order to elucidate magnetoreception in honeybees. It is premature to draw too many conclusions from the present data.

Chin-Yuan Hsu
Chia-Wei Li
Institute of Life Science, National Tsing Hua University, Hsinchu, Taiwan, Republic of China

REFERENCES

1. C.-Y. Hsu and C.-W. Li, *Science* **265**, 95 (1994).
2. D. A. Kuterbach and B. Walcott, *J. Exp. Biol.* **126**, 389 (1986).
3. ———, *ibid.*, p. 375.
4. C.-Y. Hsu and C.-W. Li, *ibid.* **180**, 1 (1993).
5. J. L. Kirschvink, *Bioelectromagnetics* **10**, 239 (1989).

24 October 1994; revised 5 June 1995; accepted 27 July 1995